



UDC 536.5

# Study of an improved copper fixed point using the LP4 Linear Pyrometer

R. Serhiienko, R. Pushchyn, V. Skliarov

National Scientific Centre "Institute of Metrology", Myronosytska Str., 42, 61002, Kharkiv, Ukraine  
rymma.sergiyenko@metrology.kharkov.ua

## Abstract

Since 1994, the National Scientific Centre "Institute of Metrology" has maintained and used the state primary measurement standard of the unit of temperature by radiation (DETU 06-03-96), which is the upper link of the traceability chain for non-contact temperature measuring instruments in the range from 1357.7 to 2800 K. One of the components of the standard is the copper fixed point, which is a cylindrical graphite crucible with a fixed point of metal – pure copper.

The condition of the metal fixed point and graphite elements was naturally affected over the period of operation of the standard, which necessitated their improvement. In addition, other components of the state were improved or completely upgraded – the irradiator (the furnace for the fixed point), argon protection and temperature control systems, and the standard pyrometer.

The purpose of this study is to confirm the metrological characteristics of the state measurement standard in terms of the realization of the copper fixed point temperature following the modernization of the standard. An overview of the experimental equipment, measurement procedures, obtained results, and the corresponding uncertainty budget are provided.

**Keywords:** state measurement standard; linear pyrometer; freezing plateau; fixed point.

Received: 21.10.2025

Edited: 01.12.2025

Approved for publication: 05.12.2025

## 1. Introduction

In the range above 1234.93 K, the reproducibility of the International Temperature Scale, ITS-90, is based on the realization of the freezing temperatures of pure metals – the fixed points of silver, gold, and copper [1].

A fixed point is a graphite crucible, usually of cylindrical shape, filled with a pure metal, which, by its design, has a blackbody cavity.

The graphite crucible is placed in the working space of a furnace, whose heating and cooling temperature regimes allow for the realization of the freezing phase transitions of a pure metal, which are identified by optical, i.e., non-contact, methods, and which serve as the basis for further extrapolation of the temperature scale according to Planck's Law.

In Ukraine, the ITS-90 is realised by non-contact methods in the range from 1357.7 to 2800 K using the state primary measurement standard of the unit of temperature by radiation (DETU 06-03-96, hereinafter – the state standard), which is maintained and used at the National Scientific Centre "Institute of Metrology"

[2, 3]. The state standard was developed based on the copper fixed point and put into operation in 1994. This experimental study was carried out at the National Scientific Centre "Institute of Metrology" with the aim of confirming the characteristics of the standard in terms of the realization of the copper fixed point temperature following the modernization of the standard.

## 2. Experimental equipment and measurement procedures

### 2.1. Description of the fixed point

#### 2.1.1. Metal purity

In the ideal approximation, the temperature of the freezing fixed point shall characterize the phase transition of a pure single-component substance. However, real materials are not absolutely pure. Table 1 shows the composition and concentrations of impurities in the copper that has been used in the state standard since 1994.

Summing up the concentrations of the impurities results in a total value not exceeding  $4.1 \times 10^{-3}\%$ , and the metal purity was 99.996%. The estimate of the uncertainty associated with metal impurities was 30 mK

based on the results of international comparisons [4]. Reducing impurity concentrations affects the properties of the metal fixed point and, consequently, the value of the reproduced temperature and corresponding uncertainty [5]. One of the tasks of modernizing the state standard was to equip it with a copper fixed point with a purity of not less than 99.9999%. Table 2 shows the data from the certificate of analysis of impurities in the metal of the improved fixed point. The analysis was carried out using the glow discharge mass spectrometry method.

Table 1  
Composition and concentration of impurities in the copper fixed point used since 1994

	Impurities	Concentration, not more than, %
1	Sb (Antimony)	$6 \times 10^{-4}$
2	Pb (Lead)	$2 \times 10^{-4}$
3	Sn (Tin)	$2 \times 10^{-4}$
4	As (Arsenic)	$4 \times 10^{-4}$
5	Bi (Bismuth)	$3 \times 10^{-4}$
6	Zn (Zinc)	$4 \times 10^{-4}$
7	Mn (Manganese)	$3 \times 10^{-4}$
8	Mg (Magnesium)	$3 \times 10^{-4}$
9	Si (Silicon)	$3 \times 10^{-4}$
10	Ni (Nickel)	$6 \times 10^{-4}$
11	Fe (Iron)	$5 \times 10^{-4}$

Table 2  
Composition and concentration of impurities in the metal of the improved fixed point

	Impurities	Concentration, not more than, %
1	Al (Aluminum)	$0.012 \times 10^{-4}$
2	C (Carbon)	$0.14 \times 10^{-4}$
3	Cl (Chlorine)	$0.003 \times 10^{-4}$
4	Fe (Iron)	$0.02 \times 10^{-4}$
5	I (Iodine)	$0.009 \times 10^{-4}$
6	K (Potassium)	$0.005 \times 10^{-4}$
7	Li (Lithium)	$0.001 \times 10^{-4}$
8	Mn (Manganese)	$0.005 \times 10^{-4}$
9	Na (Sodium)	$0.001 \times 10^{-4}$
10	S (Sulfur)	$0.015 \times 10^{-4}$
11	Ti (Titanium)	$0.006 \times 10^{-4}$

The total impurity concentration does not exceed  $0.217 \times 10^{-4}$  %, and the copper purity is 99.9999 %.

### 2.1.2. Crucible

As part of the standard modernization, a new design of the graphite crucible for the copper fixed point was manufactured. The crucible is made of a carbon-carbon composite – fine-grained graphite with a pyrocarbon binder. The purity of the composite corresponds to class OSCh-7-3. To protect against oxidation, the crucible is placed in a graphite protective shell, unlike the previous version of the fixed point, where the protective shell was made of stainless steel. Table 3 shows the main characteristics of the crucible and the protective shell.

Table 3  
Characteristics of the graphite crucible and the protective shell

Design	Cylindrical shape
Crucible	
Length x outer diameter, mm	158×41
Cavity length x inner diameter, mm	108×12
Cavity opening diameter, mm	3.0
Opening area, mm <sup>2</sup>	7.1
Cavity wall thickness, mm	3.0
Metal volume, cm <sup>3</sup>	50.9
Metal weight, g	456
Protective Shell	
Length x outer diameter, mm	200×58
Inner diameter, mm	42

Fig. 1 shows a sketch of the crucible with the protective shell. The blackbody cavity has a cylindrical shape with a conical bottom with an internal angle of 120°.

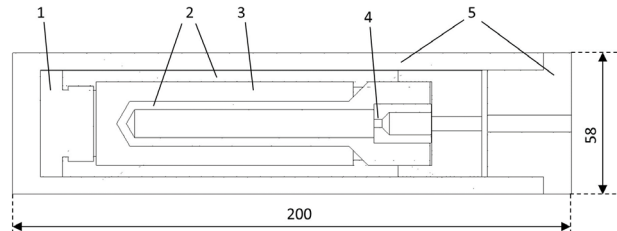


Fig. 1. Sketch of the crucible with a protective graphite shell:  
1 – graphite plug; 2 – walls of the graphite crucible; 3 – copper;  
4 – exit aperture of the blackbody cavity; 5 – graphite elements of the protective shell

Fig. 2 shows the external appearance of the crucible with a protective shell. The body of the protective shell has grooves for placing cable-type thermoelectric converters and a tube for supplying argon.

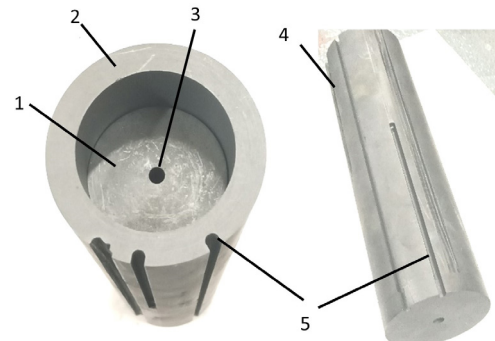


Fig. 2. The crucible with a protective shell: 1 – graphite crucible with copper; 2 – protective graphite shell; 3 – aperture of the blackbody cavity; 4 – graphite shell assembly;  
5 – grooves for thermoelectric converters

During previous studies, a so-called “crucible simulator” was used to determine the heating parameters of the fixed point. It is a graphite shell with a graphite insert, the external appearance of which is shown in Fig. 3.

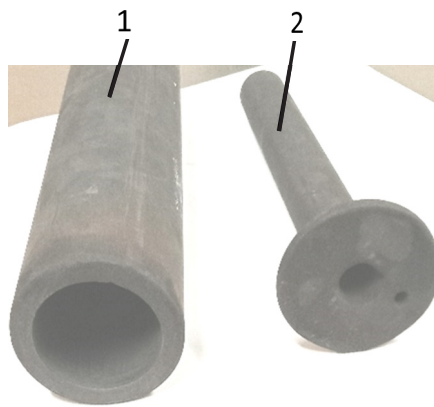


Fig. 3. The crucible simulator: 1 – graphite shell;  
2 – graphite insert

#### 2.1.3. Furnace (Irradiator)

The protective shell with the graphite crucible is placed in the ceramic tube of the “Promin-V/1350” irradiator, which is part of the state measurement standard DETU 06-03-96. The ceramic tube has three heating windings made of “Kanthal A1” nichrome wire, to which electrical power is supplied via corresponding independent regulation channels. Fig. 4 shows a diagram of the irradiator in its assembled form.

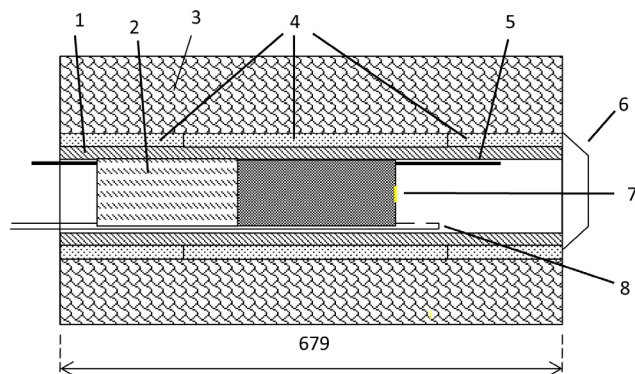


Fig. 4. Elements of the “Promin-V/1350” irradiator: 1 – ceramic tube; 2 – stationary thermal plug; 3 – thermal screen; 4 – heating windings; 5 – one of the three thermoelectric converters; 6 – exit aperture at the end face of the irradiator with a removable heat radiation plug; 7 – protective graphite shell containing the graphite crucible; 8 – tube for supplying argon

To equalize the temperature profile, a thermal screen made of fireclay brick was installed behind the protective shell with the crucible. To prevent heat loss through the front flange of the irradiator, it was thermally insulated with elements made of calcium-silicate board with a thickness of 30 mm. The operating junctions of each of the three regulating thermoelectric converters are located in the working space of the irradiator under the corresponding heating windings.

#### 2.1.4. Argon protection system

To prevent oxidation of the graphite elements and their subsequent deformation, high-purity gaseous argon in 40 l cylinders was used, with an argon volume

fraction of not less than 99.998%. Argon was supplied to the working space of the furnace through a tube made from stainless steel with an inner diameter of 3 mm. The tube was located in special grooves machined in the thermal screen and the protective graphite shell. The gas flow rate was regulated using a brass argon flow regulator AR-40-2DM in concert with an RM-A-0.063 GUZ rotameter with a built-in regulating valve. The distance between the argon exit hole into the working space of the radiator and the end face of the graphite protective shell is 15 mm. During the study, argon was supplied at temperatures above 450 °C.

#### 2.1.5. Temperature control system

The temperature control system includes OWEN TRM-101 temperature controllers (measuring-regulating devices) together with three cable-type Chromel-Alumel (Type K) thermoelectric converters (hereinafter – TCs). Using response across the three heating zones (regulation channels “2”, “3”, and “4”), electrical power is supplied to the three heating windings of the radiator. Through channel “1”, power is supplied to the thermostat of the free ends of the TCs, where a platinum sensing element with the nominal static conversion characteristic NSC Pt100 according to [5] is used as the temperature sensor.

To optimize the settings of the temperature controllers, including the values of temperature setpoints depending on time intervals, preliminary studies were carried out using a crucible simulator, which was heated to a temperature of 1090 °C. The irradiator reached a temperature of 1090 °C across all regulation channels in 250 minutes. Table 4 shows the values of temperature setpoints depending on time intervals.

Table 4  
Temperature setpoint values during preliminary studies

Temperature setpoint value, $t_{\text{set}}$ , °C	Time interval required to reach $t_{\text{set}}$ , minutes	Heating rate, °C per minute
1000	180	5.4
1080	25	3.2
1090	45	0.2

#### 2.1.6. Standard pyrometer

During the study, a precision LP4 linear pyrometer in concert with a personal computer was used. Communication with the personal computer was carried out via the RS232 serial interface. The pyrometer software (LP4DE) allows monitoring the pyrometer operation, recording the values of the pyrometer output signals, and the corresponding temperature curves. Measurements were performed at intervals of 10 s. The temperature of the pyrometer measuring head, with a silicon radiation receiver and interference filters, is stabilized at a certain value (not less than 29.0 °C) to ensure the stability of the detector output signal.

The pyrometer is equipped with three interchangeable interference filters (Table 5). In this experiment, the filter with  $\lambda = 650$  nm was used.

Table 5  
Characteristics of the LP4 pyrometer  
interference filter

Characteristic	Filters, $\lambda/\Delta\lambda$ , nm/nm		
	650/10	800/15	895/20
Maximum, nm	650	800	895
Half-width, nm	10	15	20
Transmittance value, %	72	69	70
Average effective wavelength, nm	650.2	800.1	895.1

The pyrometer was adjusted along the optical axis of the graphite crucible cavity using a fiber-optic illuminator. The focal length was 830 mm, which corresponds to a target diameter of 0.9 mm. The pyrometer position was controlled through the eyepiece, observing the pyrometer field-of-view diaphragm (Fig. 5), which shall be centred in the exit aperture of the cavity.

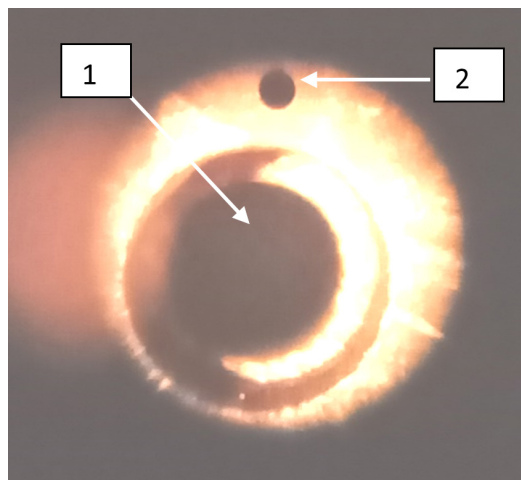


Fig. 5. Adjustment of the LP4 pyrometer: 1 – exit aperture of the cavity; 2 – field-of-view diaphragm of the LP4 pyrometer

## 2.2. Measurement procedure

Before the study, the value of dark current  $U_0$  of a standard pyrometer was verified. In the measuring range "R1" (from 1 pA to 7.95 nA), it shall be within  $\pm 0.5$  pA. During the study, the internal temperature  $t_{\text{int}}$  of the pyrometer measuring head was also verified. It shall not be less than 29.0 °C.

During the study, the temperature in the thermostat of the free ends was recorded. It reaches the set regime of 36.0 °C in 2 to 2.5 hours.

Table 6 shows the values of temperature setpoints and the approximate heating rate of the fixed point to reach 1094 °C according to the three heating zones (Fig. 6). During heating, the melting plateau of copper was also recorded. At a temperature of 1094 °C, the process was stabilized for 30 minutes.

Table 6  
Temperature setpoint values during heating of the copper fixed point

Temperature setpoint value, $t_{\text{set}}$ , °C	Time interval required to reach $t_{\text{set}}$ , minutes	Heating rate, °C per minute
950	147	6.3
1080	70	1.9
1094	45	0.3

The freezing plateau was initiated by temperature setpoints for all heating zones, the value of which was 8 °C below the phase transition temperature.



Fig. 6. Process of the "Promin-V/1350" radiator temperature reaching the 1094 °C regime

## 3. Results

Table 7 shows the measurement results for the temperature in the thermostat of the free ends of the TCs, the internal temperature of the standard pyrometer measuring head, and the value of the dark current (zero output signal) of the standard pyrometer. These measurements were performed before the start of copper melting. As it can be seen, the thermostat reached the set regime, and the parameters of the standard pyrometer are within the required limits. When processing the data for the copper freezing plateau, the value of the pyrometer dark current, obtained as the arithmetic mean of 50 observations, was accounted for.

Table 7  
The thermostat and standard pyrometer parameters

Time, h:min	Temperature setpoint for the thermostat of the free ends of the TCs, °C	LP-4 (650 nm filter)	
		$t_{\text{th}}$ , °C	$U_0$ , pA, (range "R1")
10:20	36.0	25.85	0.302
	Thermoregulator readings, °C		
10:35	37.5	26.09	0.220
11:04	35.2	27.20	0.211
11:28	36.2	27.99	0.204
12:19	36.0	28.98	0.210
13:29	36.1	29.42	0.208

Fig. 7 shows an example of the melting and freezing phase transitions of the copper fixed point in one realization, and Fig. 8 shows the freezing temperature curve on an enlarged scale. The magnitude of super-

cooling during the freezing is at the level of 1.2 °C to 1.9 °C.

The duration of the plateau for the realized transitions ranged from 11 to 30 minutes. The number of observations during the processing of experimental data ranged from 65 to 180, respectively.



Fig. 7. Example of the realization of melting and freezing of the copper fixed point

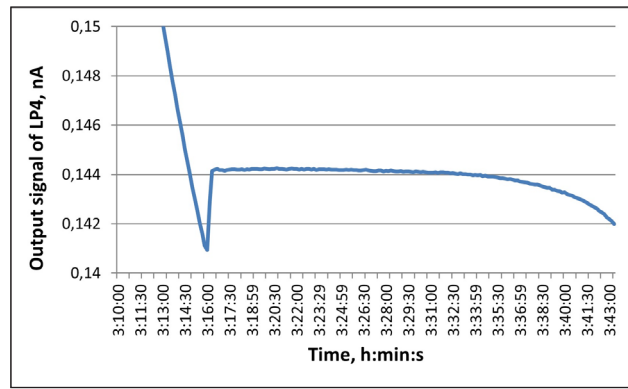


Fig. 8. Experimental temperature curve of the freezing phase transition of the copper fixed point

For the transformation of the experimental data processing results for the plateau into a temperature equivalent, the value of the increment (derivative) of the standard pyrometer calibration characteristic  $I = f(T)$  around the temperature of the copper fixed point is required. This parameter was determined three times, both during heating and during cooling of the fixed point, and the result taken was the arithmetic mean of six values (Table 8). The estimate of the pyrometer dark current in the temperature equivalent around the copper fixed point, calculated based on the  $dI/dT$  value, is 114 mK.

The experimental data for the freezing plateau were processed by two methods according to [6], having assessed the convergence between them. The first method involves removing the initial and final 15% of the plateau, and the reproducible temperature value (output signal of the standard pyrometer) is determined as the average value calculated within the remaining 70% of the readings. According to the second method,

the reproducible value of the fixed point temperature is considered to be the temperature corresponding to a certain fraction of the melt. In the second method, 50%, i.e., the first half of the plateau, was taken for the processing. Table 9 shows an example of processing one of the freezing plateaus by the two methods. As it can be seen, the convergence between the two methods is 0.5 mK. The magnitude of the plateau slope indicates the effects from impurities in the metal on the fixed point temperature to some extent. The negative sign of the plateau slope in the second method suggests the incorrectness of using only 50% of the plateau for calculating this parameter.

Table 8  
Determination of the increment of the standard pyrometer calibration characteristic around the temperature of the copper fixed point

$\Delta I$ , nA	$\Delta T$ , °C	$dI/dT$ , nA/°C (range from 1 pA to 7.95 nA)
During the heating process		
0.004886	2.847	0.001716
0.004998	2.826	0.001769
0.005165	2.919	0.001769
During the cooling process		
0.001652	0.937	0.001763
0.002134	1.224	0.001743
0.001963	1.141	0.001720
Average value ( $n = 6$ )		0.001748

Table 9  
Results of processing the experimental data on the freezing plateau of the copper fixed point

	Method 1	Method 2
Number of observations	45	32
Average value of the pyrometer output signal, nA	0.144012	0.144011
Standard uncertainty of Type A, nA	$0.260993 \times 10^{-5}$	$0.386963 \times 10^{-5}$
$dI/dT$ , nA/°C	0.001748	
Standard uncertainty of Type A, mK	1.5	2.2
Plateau slope, mK	7	-25
Range of values on the plateau, mK	45	62
Convergence of methods, mK	$ 0.144012 - 0.144011  / 0.001748 = 0.5$	

Table 10 shows the results of experimental data processing for three reproductions of the copper freezing plateau.

#### 4. Uncertainty budget

The combined standard uncertainty of the realization of the phase transition temperature of the copper freezing fixed point is calculated using the formula:

Table 10

Results of experimental data processing for three reproductions of the copper freezing plateau

Plateau realization number	Average value of the pyrometer output signal, nA	Standard uncertainty according to type "A", nA	$dI/dT$ , nA/°C	Standard uncertainty according to type "A", mK
1	0.144010	1.36814×10 <sup>-5</sup>	0.001748	7.8
2	0.144036			
3	0.144017			
Average value, nA, $n = 3$	0.144021			

Table 11

Uncertainty budget for the realization of the copper freezing phase transition temperature

Uncertainty components	Standard uncertainty, mK, 2013	Standard uncertainty, mK, 2025
	Type A	Type A
Repeatability of the value $I_{90}$	72.0	10.0
	Type B	Type B
<b>Realization of copper freezing plateau</b>		
Impurities	30.0	10.0
Emissivity	20.0	20.0
Plateau identification	5.0	5.0
Temperature difference in cavity walls, heat transfer processes	10.0	10.0
<b>Standard comparator/pyrometer</b>		
Adjustment	50.0	25.0
Spectral parameters	55.0	55.0
Source size effect	60.0	45.0
Drift (instability)	20.0	10.0
Resolution	5.0	3.0
Standard Uncertainty, mK	127.1	80.7
Expanded Uncertainty, mK ( $k = 2$ )	254.2	161.4

$$u = \sqrt{u_A^2 + u_B^2}, \quad (1)$$

where  $u_A$  is the standard uncertainty of Type A in the temperature equivalent (Table 10);  $u_B$  is the standard uncertainty of Type B, which includes uncertainties associated with the copper fixed point and the standard pyrometer as components [7].

The estimates of the components of the uncertainty budget for the realization of the freezing phase transition temperature, performed according to [7], for the improved copper fixed point are given in Table 11. For comparison, Table 11 also provides estimates of the components of the standard uncertainty obtained during the international comparisons of the DETU 06-03-96 state standard at the copper fixed point [8] in 2013.

## 5. Conclusions

The characteristics of the state standard in terms of the realization of the copper fixed point temperature were studied on the state primary measurement standard of the unit of temperature by radiation (DETU 06-03-96). During the study, the components of the state standard – graphite crucibles, pure

copper, the furnace (irradiator), argon protection and temperature control systems, and the standard pyrometer – which were improved or completely upgraded as part of the work on the modernization of the state standard – were used.

The results of the study show that after the modernization of the state standard, the Type A standard uncertainty, due to the repeatability of the freezing plateau, does not exceed 10 mK, which is a significantly smaller value compared to the results obtained during the international comparisons in 2013 [8]. The replacement of the fixed point with copper of 99.9999% purity also reduced the Type B uncertainty component associated with the concentration of impurities in the metal. The use of the precision LP-4 linear pyrometer during the recording of the freezing plateau affects both the value of the Type A uncertainty and the Type B uncertainty components due to factors such as pyrometer adjustment, source size effect, instability, and resolution. Thus, the value of the expanded uncertainty of the realization of the copper freezing phase transition temperature has been reduced by almost 40% compared to 2013 [8], which fully confirms the metrological characteristics of the state standard.

# Дослідження вдосконаленої реперної точки міді із застосуванням лінійного пірометра LP4

Р.П. Сергієнко, Р.В. Пущин, В.В. Скляров

Національний науковий центр "Інститут метрології", вул. Мироносицька, 42, 61002, Харків, Україна  
gymta.sergiyenko@metrology.kharkov.ua

## Анотація

З 1994 р. в ННЦ "Інститут метрології" зберігається та застосовується державний первинний еталон одиниці температури за випроміненням ДЕТУ 06-03-96, який є верхньою ланкою схеми простежуваності для безконтактних засобів вимірювання температури в діапазоні від 1357,7 до 2800 К. Одним зі складових елементів державного еталона є реперна точка міді, яка являє собою графітовий тигель циліндричної форми з реперним металом – чистою міддю. Час експлуатації еталона закономірним чином впливув на стан реперного металу та графітових елементів, що обумовило необхідність їх оновлення. Крім того, проведено доопрацювання або повне оновлення інших складових елементів державного еталона – випромінювача (печі для реперної точки), систем аргонового захисту та регулювання температури, еталонного пірометра.

Метою дослідження є підтвердження метрологічних характеристик державного еталона в частині реалізації температури реперної точки міді після проведення робіт з удосконалення державного еталона.

Наведено опис оновленої реперної точки міді. Розглянуто конструкцію вдосконаленого графітового тигля із захисною оболонкою. Наведено схему печі для реперної точки міді. Описано системи аргонового захисту та контролю температури. Наведено процедуру вимірювань за допомогою лінійного пірометра LP4. Надано результати реалізації температури фазового переходу тверднення реперної точки міді. Розглянуто методику визначення приросту градуувальних характеристик еталонного пірометра LP4 навколо температури реперної точки міді. Розглянуто два методи обробки експериментальних даних на плато тверднення для визначення вихідного сигналу еталонного пірометра. Наведено оцінку стандартної невизначеності за типом А для кількох плато. Подано бюджет невизначеності для реалізації температури фазового переходу тверднення міді.

**Ключові слова:** державний еталон; лінійний пірометр; плато тверднення; реперна точка.

## References

1. Guide to the Realization of the ITS-90. Fixed Points for Radiation Thermometry. BIPM, 2018. Available at: [https://www.bipm.org/utils/common/pdf/ITS-90/Guide\\_ITS-90\\_2\\_5\\_RTFixedPoints\\_2018.pdf](https://www.bipm.org/utils/common/pdf/ITS-90/Guide_ITS-90_2_5_RTFixedPoints_2018.pdf)
2. Stvorennia pervynnoho etalona odynytsi temperatury kelvina za vyprominiuvanniam v diapazoni 1357.77–2800 K [Creation of the primary standard of the Kelvin temperature unit by radiation in the range of 1357.77–2800 K]. Research report, no. state reg. IA01006770R, Kharkiv, 1994. 113 p. (in Ukrainian).
3. Nazarenko L.A., Belykh V.V., Kysil O.M. et al. Derzhavnyi pervynnyi etalon odynytsi temperatury Kelvina za vyprominiuvanniam v diapazoni 1357.77–2800 K [State primary standard of the Kelvin temperature unit by radiation in the range 1357.77–2800 K]. *Ukrainian Metrological Journal*, 1995, no. 1, pp. 26–30 (in Ukrainian).
4. Fellmuth B., Hill K.D., Pearce J.V., Peruzzi A., Steur P.P.M., Zhang J. Guide to the Realization of the ITS-90. Fixed Points: Influence of Impurities. Available at: file:///C:/Users/user/Downloads/Guide\_ITS-90\_2\_1\_Impurities\_2018.pdf
5. DSTU 2858:2015. Termoperetvoriuvachi oporu. Zahalni tekhnichni vymohy i metody vyprovuvannia [Thermo-converters of resistance. General technical requirements and test methods]. Kyiv, 2015 (in Ukrainian).
6. DSTU 4017-2001. Metrolohiia. Shkaly temperaturni [Metrology. The temperature scales]. Kyiv, 2001 (in Ukrainian).
7. CCT/03-03. CCT-WG5 on radiation thermometry. Uncertainty budgets for realisation of scales by radiation thermometry. BIPM, 2003. Available at: <https://www.bipm.org/documents/20126/28438732/working-document-ID-775/b5219f09-2504-ec12-724b-32374500575a>
8. Realizations of the ITS-90 at 1084.62 °C. BIPM, 2014. Available at: <https://www.bipm.org/kcdb/comparison?id=1038>